Entanglement relaxation time of polyethylene melts from high-frequency rheometry in the mega-hertz range

Levente Szántó, Robert Vogt, Julia Meier, Dietmar Auhl, Evelyne Van Ruymbeke, and Christian Friedrich

Citation: Journal of Rheology **61**, 1023 (2017);
View online: https://doi.org/10.1122/1.4998174
View Table of Contents: http://sor.scitation.org/toc/jor/61/5
Published by the The Society of Rheology

Entanglement relaxation time of polyethylene melts from high-frequency rheometry in the mega-hertz range[a)]

Levente Szántó and Robert Vogt

Freiburg Materials Research Center (FMF), Albert-Ludwigs-University of Freiburg, Stefan-Meier-Street 21, D-79104 Freiburg, Germany and Institute for Macromolecular Chemistry, Albert-Ludwigs-University of Freiburg, Stefan-Meier-Street 31, D-79104 Freiburg, Germany

Julia Meier

Freiburg Materials Research Center (FMF), Albert-Ludwigs-University of Freiburg, Stefan-Meier-Street 21, D-79104 Freiburg, Germany

Dietmar Auhl

Faculty of Humanities and Sciences, Maastricht University, Kapoenstraat, 26211 KW Maastricht, The Netherlands

Evelyne Van Ruymbeke

Bio- and Soft Matter (BSMA), Institute of Condensed Matter and Nanosciences, Université catholique de Louvain, Croix du Sud 1, Louvain-la-Neuve B-1348, Belgium

Christian Friedrich[b)]

Freiburg Materials Research Center (FMF), Albert-Ludwigs-University of Freiburg, Stefan-Meier-Street 21, D-79104 Freiburg, Germany and Institute for Macromolecular Chemistry, Albert-Ludwigs-University of Freiburg, Stefan-Meier-Street 31, D-79104 Freiburg, Germany

(Received 2 February 2017; final revision received 21 July 2017; published 17 August 2017)

Abstract

The determination of relevant rheological properties and parameters in a very broad frequency range can be achieved for a number of thermoplastic polymers, for example, polystyrene, by applying the time-temperature-superposition principle. In contrast, polyethylene can only be explored rheologically in a limited frequency range, due to its fast crystallization below the crystallization temperature and its weak viscosity temperature-dependence. In this paper, various commercially available polydisperse and narrowly distributed linear and branched polyethylenes and ethylene-vinylacetate-copolymers were characterized. A piezoelectric- and a new quartz (crystal resonator) rheometer (QR) with an extended frequency range were utilized for the characterization. Introduction of high frequency rheological techniques and implementation of these new measurement methods are shown. For the first time, the entanglement relaxation time in the higher MHz frequency range was determined by applying the QR-technique and compared with those obtained by an alternative experimental method and numerical calculations. © *2017 The Society of Rheology*. [http://dx.doi.org/10.1122/1.4998174]

I. INTRODUCTION

The determination of the dynamic moduli G' and G'' in a very broad frequency range can be achieved for many thermoplastic polymers by applying the time-temperature-superposition (TTS) principle. For thermorheologically simple materials such as amorphous atactic polystyrene, the covered frequency range might spread over all relaxation regions, from the terminal region up to the glassy region and therefore provides access to all important parameters of linear viscoelasticity.

When TTS is applicable in a wide frequency and temperature range, the dynamic moduli master curves exhibit two (or even three) important crossovers, which provide links to structural and dynamic characteristics of polymer chain. The zero shear viscosity η_0 and the first crossover frequency ω_x or terminal relaxation time $\tau_t \approx 1/\omega_x$ are related to the size and size distribution of the linear molecule, while the second crossover frequency ω_{2x} (it marks the end of the plateau region), the corresponding entanglement relaxation time $\tau_e \approx 1/\omega_{2x}$, and the entanglement modulus G_e give access to an

[a)]This paper is dedicated to the Late W. Pechhold and A. Kirschenmann, who developed and built the used quartz rheometer.

[b)]Author to whom correspondence should be addressed; electronic mail: chf@fmf.uni-freiburg.de

entanglement molar mass M_e and monomeric friction coefficient ξ_0.

The entanglement relaxation time τ_e is the Rouse time of a part of a chain, which corresponds to entanglement spacing, defined as

$$\tau_e = \left(\frac{M_e}{M_0}\right)^2 \frac{\xi_0 b^2}{3\pi^2 k_B T}, \quad (1)$$

where b is the statistical segment length of a Gaussian polymer chain, M_0 is the molecular mass of the monomer unit, k_B is Boltzmann constant, and T is temperature.

While the main structural parameter b can be determined by different scattering, and even viscometric techniques, the main dynamic characteristic ξ_0 can be accessed through the entanglement relaxation time τ_e which makes the experimental determination of this parameter so important. Alternative methods for the determination of ξ_0 and τ_e can be found in the papers by Pearson *et al*., Luettmer-Strathmann and van Meerveld [1–3], and others.

Ferry [4], who was one of the first to deal with this subject, defined empirically the constructed crossover between G'' curve and the horizontal plateau modulus (G_N^0) line as $\omega_e = 1/\tau_e$, given in Eq. (2)

$$\omega_{G_N^0 \times G''} = \omega_e = \frac{1}{\tau_e}. \quad (2)$$

Liu [5] confirmed this approach by discovering and analyzing the so called monomer density re-equilibration peak. In doing so, he set Ferry's approach on a molecular basis and showed that the frequency at which the maximum of this peak is present is identical to the equilibration time τ_e. Moreover, Liu *et al*. considered still another possibility to determine τ_e, namely, from the experimental data of ω_{2x} using Eq. (3). By evaluating various entangled polymers such as polybutadiene, polyisoprene, and polybutylene, they established the ratio between ω_{2x} and ω_e

$$\omega_e = \frac{\omega_{2x}}{3}. \quad (3)$$

Due to the fact that τ_e determined by this method is related to experimental data in the ω_e frequency range, this is an experimental approach (technique) [4,5].

Another approach to determine τ_e is related to the use of material functions or material parameters originating from the terminal relaxation region. Due to the fact that these methods rely on the existence of reliable equations (models) which connect these parameters or frequency ranges, this is a calculation approach [6–8].

Pattamaprom and Larson [7] developed a model to determine the entanglement relaxation time τ_e from dual-constraint and double reptation models for monodisperse and polydisperse polymers. The entanglement relaxation time τ_e can be determined from the zero-shear viscosity η_0, according to the following equation:

$$\tau_e = \frac{\eta_0}{C_1 G_N^0 \left(\frac{M_w}{M_e}\right)^{3,4}}, \quad (4)$$

where C_1 is a constant which does not depend on the chemical composition of the polymer or on the temperature and it is equal to 0.051, G_N^0 is the plateau modulus, and M_w is the weight-average molecular weight of the polymer.

Another method, also related to the measurement of rheological properties pertinent to the terminal relaxation region, was reported by Ramos *et al*. [6]. They used a simplified reptation model combined with a model describing contour length fluctuation. According to their model, the entanglement relaxation time τ_e is accessible through terminal relaxation time τ_t of a chain with molecular mass M_i, using

$$\tau_e = \frac{\tau_t}{3} \cdot \left(\frac{M_e}{M_i}\right)^3 \cdot \left(1 - \kappa \cdot \left(\frac{M_e}{M_i}\right)^{0.5}\right)^{-2}. \quad (5)$$

Here, κ is a coefficient which is used according to Likthman and McLeish [9] calculation and it is equal to 1.69.

A last approach relies on the use of simulation techniques, applying Monte Carlo and/or molecular dynamics simulations [6,10].

While the mentioned procedures were successfully applied to many different polymers, the experimental determination of τ_e for polyethylene (PE) is missing for the following reasons.

For semicrystalline polymers such as PE or isotactic polypropylene (iPP) only the terminal relaxation region and a transition region to the rubbery plateau can be explored and the corresponding TTS is very limited. The main reasons for the limitation of accessible frequency range are high crystallization rate of these polymers and the restrictions concerning frequency ranges of commercially available rheometers (CR). However, there is a need for rheological data in the high-frequency regime for semicrystalline polymers, for which the TTS principle is limited or not applicable. The problem may be solved by employment of high frequency rheometers at temperatures above crystallization $T > T_c$.

Although the design principles for the rheometers allowing higher frequencies up to and beyond the MHz ranges (see [11] for details) are known, not a single rheometer is commercially available to make these measurements on polymer melts. In a previous paper, Kirschenmann and Pechhold [12] presented and tested a rheometer which works in the rotary shear mode and covers a frequency range from 0.5 to 2 kHz due to its piezoelectric actuation. The authors found this piezo-rotary-vibrator (PRV) suitable for measuring linear viscoelastic properties of such polymer melts as polysiloxanes at ambient temperatures and polycarbonates and polyamides for temperatures up to 533 K. A similar instrument, originating from the Pechhold group as well, allows even higher frequencies in kHz, but is restricted to polymer dispersions and solutions [13].

To enter the plateau region for PE melts, a technique that allows the rheometer to operate in the MHz range and beyond is required. Such an instrument, a so called quartz resonator (QR), was presented by Theobald *et al*. [11] and was found suitable for silicon oil and other low glass transition temperature (T_g) polymers. Materials, which are soluble,

dispersed, or melt at ambient temperatures, can be characterized by quartz crystal resonators. The details of experimental setup and the operation of this QR will be presented in the experimental part of this paper.

The fundamental operation principle of the QR is identical to that of the widely used quartz-crystal microbalances (QCM), which were designed to operate at one frequency, in contrast to the QR. QCM sensors can be used to measure viscosity, mass, and contact forces [14–17]. A profound description of QCM and its operation of different modes and aspects are detailed by Johannsmann in [18]. There are reports that [19–23] describe the use of QCM as a sensor to follow the changes of polymeric material with time. However, the use of QCM as a rheometric tool for polymer melts is missing.

In this study, we adopt the existing rheometer techniques, PRV and QR, to the needs of a proper rheological characterization of polymer melts in general and PEs in particular. Using conventional rheometry and high frequency techniques, we determined the rheological behavior of various PE samples in the broadest frequency range possible, including the MHz range (shown in Fig. 1), in order to derive important rheological parameters such as the entanglement relaxation time. Amorphous poly(vinyl acetate) (PVAc) and poly(ethylene-*co*-vinyl acetate) (EVA) copolymer samples, which interlink the PVAc and the PE samples, were used to demonstrate the suitability of the PRV and especially of the QR, and to highlight the transition of material parameters from one polymer to another. The experimental determination of the entanglement relaxation time of PE is the main goal of the present paper. The experimental τ_e-values were compared to the τ_e-values determined by alternative methods given in the literature.

II. EXPERIMENT

A. Materials

Molecular data and melting temperatures of the polymers under investigation are given in Table I. Most of the polymers are of industrial grade, and the molecular data are taken from the supplier. Samples from industrially available polymer were directly prepared without any additional modification. Our laboratory scale high density PE (HDPE) samples (HDPE 340 and 500; see Table I for details) were stabilized by using a modified method of Kukalyekar *et al*. [26]. These polymer samples were mixed in an acetone solution with 2 wt. % of a stabilizer mixture consisting of Irganox 1010 and Irgafos 168 in a ratio of 1:4. After 15 minutes in an ultrasonic bath, the sample was dried overnight in a vacuum oven at 333 K.

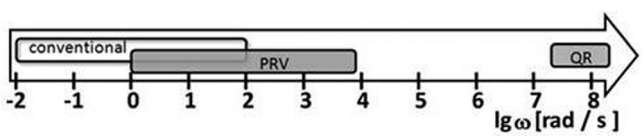

FIG. 1. Schematic of the typically accessible frequency range covered in the oscillatory mode by conventional rheometers (conventional), PRV, and MHz QR.

TABLE I. Molecular data and melting temperatures of the polymers under investigation. n.d., not determined.

Polymer/sample code	M_w[a] (kg/mol)	M_w/M_n[a]	T_c[b] (K)
PVAc/EVA100	61	5	308
EVA40[c]	130	30	316
EVA9[c]	200	30	372
LLDPE/EVA0[d]	150	3.4	396
LDPE[e]	240	14	381
HDPE 340[f]	340	1.2	n.d.
HDPE 500[f]	500	1.3	n.d.

[a]As determined from GPC (apart from EVA).
[b]T_c is the characteristic temperature; for amorphous polymers shows the T_g and for crystalline ones the T_m.
[c]The melting temperature of EVA are taken from paper [24] and M_w, M_w/M_n are retrieved from the best fit of the experimental data. (For details see supplementary material [29]. Forty and nine after EVA represents the PVAc content in wt. %.)
[d]This linear low density polyethylene (LLDPE) was commercialized under the trade name "Escorene 1201" and can be found under the name "Exxonmobil LLDPE LL 1201 XV" now
[e]The investigated low density polyethylene (LDPE) is Lupolen 1840 H.
[f]These HDPEs were synthesized in house by Kurek [25].

The samples for rheological characterization were prepared in a hot press at 463 K under vacuum and 25 bar pressure. For the conventional rheological measurements, we used sample disks with a diameter of 25 mm and a height of about 1 mm. In the case of the two other rheometers, the polymer powder was molded via the same hot press procedure in plate, with a thickness of about 1 mm, which was cut in pieces with circular diameters of 40 mm for the PRV or 8 mm in the case of the QR.

B. Conventional oscillatory rheometry

The rheological experiments in oscillatory shear mode were performed on a strain-controlled advanced rheometric expansion system rheometer (TA instruments) equipped with a 2K FRTN-1 transducer. The rheological tests were carried out in a nitrogen atmosphere using 25-mm parallel-plate geometry. The frequency sweeps were conducted at various temperatures in the linear viscoelastic regime. Isotherms were shifted horizontally to master curves using the shifting program lstemp [27] and IRIS of Winter and Mours [28].

C. Piezoelectric rotary vibrator (PRV)

The piezoelectric rotary vibrator (PRV) was developed by Kirschenmann *et al*. [12] at the University of Ulm. This piezoelectric rheometer determines moduli in a frequency range from 0.5 Hz up to 2 kHz in dynamic shear mode (see Fig. 1). Due to this, the PRV enlarges the accessible frequency range of the conventional rheometers to higher frequencies. A 40 mm parallel plate geometry was used, and all experiments were run within a nitrogen atmosphere to prevent degradation of the polymer. The lowest operation temperature was set by a nitrogen cooling device at approximately 143 K and an upper temperature is limited by applying an electrical heating up to 573 K.

D. Quartz resonator

A prototype of the QR was developed by Theobald *et al.* [11]. The MHz QR (see Fig. S2 in supplementary material [29]) consisted of 3 MHz AT-cut thickness shear quartz, which allowed the determination of shear moduli G^* at 3 MHz with three overtones: 9, 15, and 21 MHz. The quartz crystal itself consisted of SiO_2 with gold electrodes on the surface. The sample must completely cover the gold electrode. The thickness of the QR sample must be larger than $20{\cdot}\delta$, where δ is the penetration depth of the shear wave. Its value changes from the highest frequency of $\sim$0.1 μm to the quartz's base frequency of $\sim$3 μm. Thus, the thickness of the sample fulfills the condition of a semi-infinite medium [30]. The measurements were carried out at a temperature range of 343 K to 503 K without nitrogen atmosphere. The measurement was controlled by a computer, which was also connected to a temperature controller and heating device. The excitation of the resonance curve and analysis of experimental data were performed by a network analyzer (SN-2 from Wandel & Goltermann). A detailed description of the QR set-up, measurement, and evaluation of the gathered data can be found in the supplementary material [29].

E. Molecular modeling

For the molecular modeling of the rheological data, the tube-theory based model of van Ruymbeke *et al.* [31,32] [the time marching algorithm (TMA)] was employed. This has been successfully validated also for polydisperse samples. The model accounts for different relaxation mechanisms such as reptation, constraint release, and contour-length fluctuations [33,34]. The fact that fast motions of surrounding chains at the observed time scale can lead to an acceleration of the relaxation processes is taken into account by the dynamic tube dilution concept [35,36].

In this model, the relaxation modulus as a function of time, $G(t)$, accounts for both the high frequency Rouse process, $G_R(t)$, and the disentanglement modulus $G_d(t)$ [31]

$$G(t) = G_{\mathrm{R}}(t) + G_{\mathrm{d}}(t), \tag{6}$$

with

$$G_{\mathrm{R}}(t) = \sum_k \frac{\upsilon_k \rho RT}{M_k} \left\{ \frac{1}{4} \sum_{p=1}^{Z_k} \exp\left(-\frac{p^2 t}{\tau_{\mathrm{R}}(M_k)} \right) + \sum_{p=Z_k+1}^{n} \exp\left(-\frac{2p^2 t}{\tau_{\mathrm{R}}(M_k)} \right) \right\}. \tag{7}$$

In Eq. (7), υ_k and $\tau_R(M_k)$ represent the weight fraction and the Rouse time of chain with a molar mass M_k, respectively. Z_k represents the number of entanglements in a chain k; the parameter ρ is the monomeric density, and R is the gas constant. Following [6], the high frequency Rouse dynamics accounts for both the fast modes related to the molecular segments shorter than M_e, and longitudinal modes, which take place within the tube. It must be noted that such description of the high frequency dynamics necessarily leads to identical storage and loss moduli at a high frequency, with a frequency dependence described by a power law with an exponent 0.5 ($G',G'' \propto \omega^{1/2}$).

On the other hand, the disentanglement modulus is defined as

$$G_{\mathrm{d}}(t) = G_{\mathrm{N}}^0 \varphi'(t) \{\phi(t)\}^{\alpha}, \tag{8}$$

with $\varphi'(t)$, being the unrelaxed fraction of initial tube segments and α, the dynamic dilution exponent. Constraint release mechanics are taken into account by the dilation factor $\phi(t)$, which defines the diameter of the dilated tube. In the case of the polydisperse samples studied here, its value is well approximated by the unrelaxed fraction of initial tube segments, $\varphi'(t)$ [31]. This last parameter is determined by looking at all molecular segments x_k of all chains k, from $x_k = 0$ at on extremity of a chain to $x_k = 1$ at the middle of the chain, and by looking at the probability that these segments are not yet relaxed through reptation or contour length fluctuations mechanisms

$$\varphi'(t) = \sum_k \upsilon_k \int_0^1 p_{rept}(x_k t) p_{fluc}(x_k t)\, dx_k, \tag{9}$$

with $p_{fluc}(x_k,t)$ and $p_{rept}(x_k,t)$ being the corresponding survival probabilities of the molecular segment x_k [31].

The fundamental model parameters needed to determine the time- or frequency dependence of rheological material functions include the entanglement modulus G_e, which is a factor of 1.2 higher than the experimentally observed rubber-elastic plateau modulus [37], the entanglement-relaxation time τ_e, and the entanglement molecular weight M_e. The dynamic dilution exponent α was set constant with a value of 1 [36–42].

Furthermore, the molecular weight distribution (MWD) taken into account to obtain the predictions was an assumed logarithmic-normal distribution.

III. RESULTS AND DISCUSSION

A. Evaluation of dynamic moduli in the MHz range

Figure 2(a) shows the master curve of PVAc (solid line) determined with the CR. The isotherms of PVAc were evaluated in an interval from 343 to 463 K. The TTS is valid in the given temperature range, and this polymer possess a strong enough temperature dependence of viscosity [similar or even stronger temperature dependency than polystyrene], which allows to cover the frequency range from the terminal region, through the plateau region until the second crossover. The measurements closer to the glass transition temperature, which corresponds to even higher frequencies, are terminated by the transducers technical capabilities.

One isotherm of PVAc taken with the PRV is presented in Fig. 2(a) as well. For clarity reasons, we plotted only that isotherm which was determined at 403 K and shifted to the reference temperature $T_{\mathrm{ref}} = 443$ K. We choose this isotherm because it contains the first crossover frequency of PVAc, and therefore allows for the most accurate "positioning."

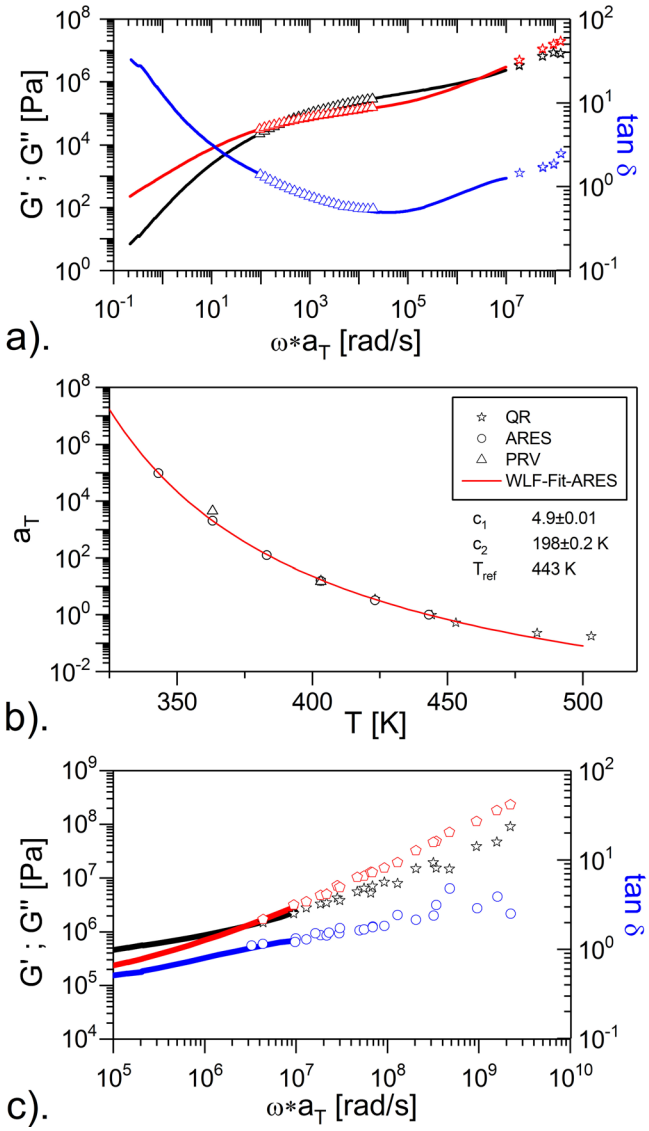

FIG. 2. (a) Dynamic moduli of PVAc vs frequency at $T_{ref} = 443$ K. The CR master curve is presented by solid lines together with one QR isotherm (stars) and the 403 K isotherm of the PRV shifted to Tref (triangle). (b) Shift factors aT of PVAc (symbols) vs temperature together with the WLF-fit (line) on the basis of CR data. (c) Dynamic moduli vs frequency in the area of overlap between the QR data (symbols) and the master curve obtained by CR (lines).

The very good agreement between moduli determined by both techniques proves the accuracy of measurement of the PRV device. Moreover, Fig. 2(a) shows the dynamic moduli of PVAc determined by QR, too. For clarity, we also plotted only one QR isotherm, which was taken at T_{ref} and plotted without any modification (shifting). More details (other isotherms) are provided in Fig. 2(c).

The shift factors, a_T, which correspond to a reference temperature of $T_{ref} = 443$ K, and which are given for the data determined by all three techniques, are shown in Fig. 2(b) as symbols. The displayed Williams–Landel–Ferry (WLF)-fit was calculated from the shift factors, which were obtained by the shifting procedure of the CR isotherms only. It can be seen that all shift factors determined by high frequency rheometry agree well with those from conventional rheometry. Only for the two highest temperatures do the QR shift factors deviate from the fit line. This might be due to the fact that the temperature calibration curve of the quartz, which was obtained before each measurement, features small systematic deviations at higher temperatures above 473 K. This deviation in the calibration curve can be caused by the temperature-frequency coupling effect. AT-cut crystals are designed in such a way that the resonance frequency is almost independent of temperature. Nevertheless, there are limits in compensation. A temperature coefficient of frequency can be performed for one temperature and one overtone at a time. Furthermore, defect-free crystals are very rare, and as a response for stress and high temperature, these defects can migrate and rearrange, influencing the crystal frequencies [18]. Moreover, Theobald *et al.* and Kirschenmann observed that with increasing temperature, the frequency of the quartz crystal slightly increases from the calibrated value [11,30]. Other reasons for inaccuracy of shift factors at temperatures higher than 473 K are presented and discussed in the supplementary material [29].

An enlarged presentation of master curves for moduli and tanδ in the region of the second crossover frequency is given in Fig. 2(c). This figure includes the master curve determined by CR (lines) and all isotherms (symbols), which were taken by the QR. As a result, a smooth transition from CR to QR data can be seen for the moduli as well as for tanδ-values. Thus, with the help of the high-frequency technique, it was possible to extend the available frequency range by more than two decades.

B. Thermorheological properties of EVA series in the MHz range

The changes appearing in the rheological properties going from the neat PVAc to the neat PE via two copolymers are discussed. Terminal properties such as zero shear viscosity are not discussed because they depend strongly on molar mass and molar mass distribution, which are different for the studied polymers.

The focus is on properties of local chain dynamics, which are independent of molar mass and are monitored in the high frequency range.

The master curves of these four polymers, which were obtained with the help of all three rheometer techniques, cover a frequency range of ten decades and are displayed in Fig. 3 (the corresponding shift factors are presented in Fig. 4). For all polymers, the linear viscoelastic properties are shown from the terminal region to the second crossover frequency and beyond. It can be observed that the second crossover shifts to higher frequencies by decreasing the vinyl acetate content. The change of crossover frequency with polymer composition can be followed in Fig. 3 (see arrows), and the values of corresponding entanglement time in dependence on vinyl acetate content can be found in Fig. 5.

Obviously, all three rheological techniques together are not sufficient to guarantee a continuous course of G^* master curve data for the two copolymers and PE. In contrast to the PVAc sample, which shows the desired continuous lines, for the latter three polymers, there is a gap between data points received on CR/PRV instruments and those from the QR

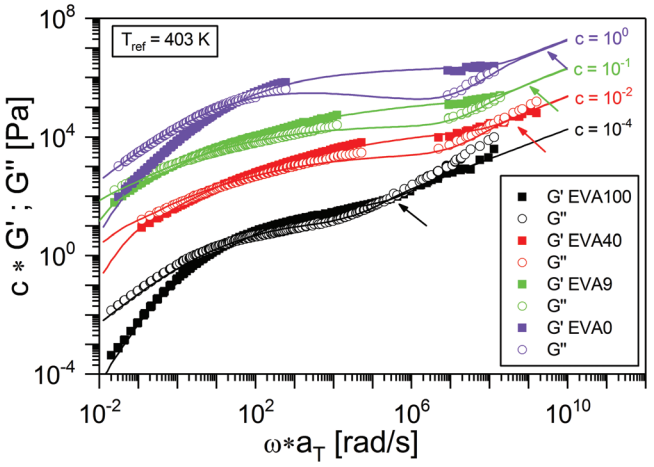

FIG. 3. Dynamic moduli of various polymer samples vs frequency; EVA100 (PVAc), EVA40, EVA9, and EVA0 (PE); the master curves have been shifted vertically by factors of 100, 10^{-1}, 10^{-2}, and 10^{-4}, respectively, for clarity. Lines are predictions of the TMA tube model for polydisperse linear polymers.

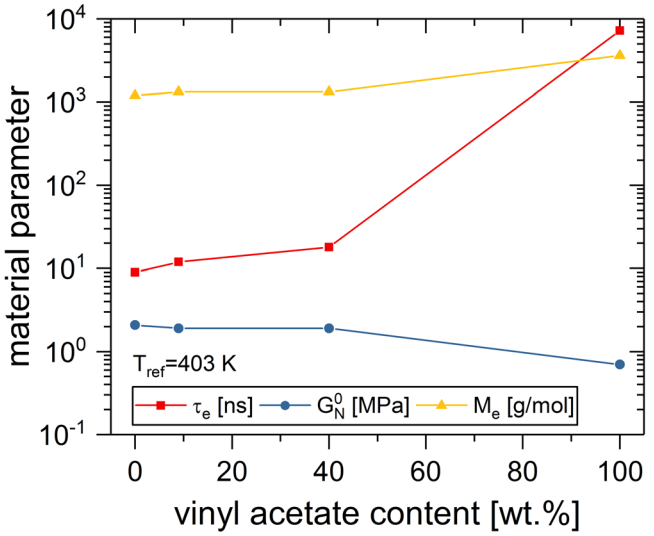

FIG. 5. Characteristic material parameters as a function of vinyl-acetate content. The straight lines are to guide the eye.

technique. It was observed that the frequency range of missing data increased with decreasing vinyl acetate content of the polymers. There are two reasons for the appearance of the gap in the data of EVA9, e.g., in comparison with EVA100. The first is related to the highest and lowest temperature, which was realized for the two polymers with QR and PRV, respectively. While the highest temperature at QR had to be decreased from 503 K for EVA100 to 443 K for EVA9 for reasons of polymer stability, the lowest temperature at PRV had to be increased from 353 to 383 K for both polymers due to crystallization. The second reason arises from the worsening of the "shiftability" of isotherms due to a much weaker temperature dependence of the shift factors of EVA9 in comparison to PVAc (see Fig. 4). Thus, a combination of the narrower temperature ranges where isotherms can be taken together and the weaker temperature dependence of shift factors cause this effect. Continuous moduli curves for PE can be only received if instruments covering the intermediate frequency range between several kHz and the MHz range (see Fig. 1) are available.

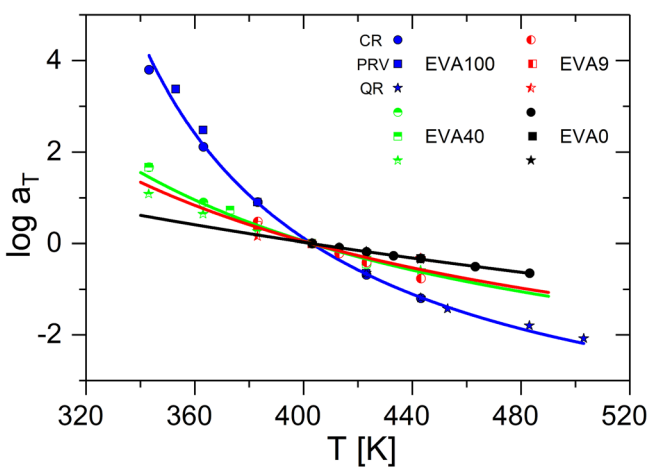

FIG. 4. Shift factors a_T determined by all three techniques for reference temperature of 403 K vs temperature. The lines represent the WLF fits determined for all data points.

Another way to follow the changes in linear viscoelastic properties of a polar polymer such as PVAc toward a nonpolar such as PE is to apply a tube model to the experimental data and to analyze the derived parameters. From given rheological data, the tube model parameters G_e and τ_e can directly and independently from each other be determined by matching the TMA tube model predictions with the vertical and horizontal positions of the ω_{2x} crossover position, respectively. Then, M_e can be determined based on the relationship between G_e and M_e (i.e., $G_e = \rho RT/M_e$), and the relaxation moduli can be predicted, based on their average molar mass and polydispersity. Using these parameters, a good "overall" agreement between data and model was found (see Fig. 3). The discrepancy observed at high frequency is attributed to the fact that the theoretical curves can only lead to a power law dependence of G' and G'', with an exponent of 0.5 [see Eq. (7)], which was not observed in the experimental data. Therefore, the value of τ_e was fixed in the model in order to minimize this discrepancy. A similar issue was recently discussed by Park *et al.* [43] in case of polybutadiene polymer melts. In order to accurately determine τ_e, the authors proposed to subtract the effects of glassy relaxation, described by the Kohlraush–Williams–Watts expressions. However, in our case, the data are too limited at high frequency to take this process into account.

On the other hand, deviations between model and experimental curves at low frequency are thought to originate from the idealized MWD data, whereas small differences can also be due to the fact that tube models still do not perfectly reflect the dynamics of entangled polymer chains. In order to achieve a better agreement, an evaluation and confirmation of the MWD data as well as the tube model parameters would be necessary. Since in the case of the statistical copolymers EVA9 and EVA40 reliable MWD data are difficult to obtain from chromatography, they have been specified in order to match the experimental data.

Figure 5 shows the dependence of the characteristic material parameters on the vinyl-acetate content. The values for

G_N^0 and M_e of PE and the copolymers are thought to vary by about 10%, whereas the determination of τ_e can result in variations of up to 50%. The value of G_N^0 can then be compared to the values from the literature: Fetters *et al.* [44] showed that the measured G_N^0 of PE is 2.08 MPa at 413 K, which corresponds to 2.05 MPa at 403 K. This value is very close to the value of 2.1 MPa that was found from the TMA fit. However, a larger discrepancy is observed for the plateau modulus of PVA, i.e., EVA100. Its value was fixed by Fetters *et al.* to be 0.35 MPa at 333 K, i.e., 0.28 MPa at 403 K, and determined here as equal to 0.7MPa. The difference between the fit and experimental value results from the low M_w of the PVAc used in the experiments (only seven times higher than M_e). In such cases, the Rouse relaxation and disentanglement mechanisms overlap, leading to an apparently higher plateau modulus.

For the EVA9 and EVA40 copolymers, the model parameters are expected not to deviate significantly from PE with change of the composition, according to Arsac *et al.* [45]. Our experimental data confirm these results.

C. *Determination and evaluation of entanglement relaxation time* τ_e of PE

Up till now, the entanglement relaxation time of PE has not been determined experimentally from the high-frequency region of rheological measurements. For the first time, it is possible to specify directly the value of τ_e using the high-frequency rheometer (QR) which operates in the MHz range. Four different PE samples (Lupolen 1840H, Escorene 1201, PE340 and PE500) were analyzed. In order to compare the obtained results with the findings of other researcher groups, the isotherms from 443 K were shifted to 463 K. The shift factor was calculated using the Arrhenius dependency ($E_a = 25$ kJ/mol). Further conversion is necessary to compare these results with the literature. The conversion of Hz to rad/s (according to $\omega = 2\pi * f$) was done. After applying the aforementioned steps the values obtained are presented in Fig. 6. The experimental data covers the second cross-over region but does not include the cross-over itself. Obviously, the frequencies at which the QR operates are still too low. However, the frequencies were high enough to determine the cross-over with acceptable accuracy (for details of error analysis see supplementary material [29]).

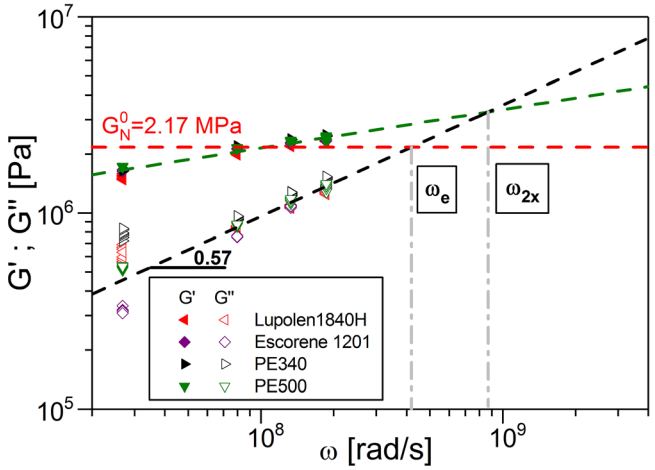

FIG. 6. QR measurements of various PE at 463 K.

To ensure the reliability of the results gained by this new rheometric measurement, the experiments were repeated, leading to a high reproducibility as shown in Fig. 6. Despite the different PE types (with or without chain branching, different MWD or M_w) all moduli superimpose well with the exception of G'' data at the crystal's fundamental frequency (3 MHz, which corresponds after temperature shift to 2.6×10^7 rad/s). The observed scatter of G'' data at this frequency is caused by the transient character of oscillation of the quartz-crystal. This is a well-known phenomenon and does not influence G' data [46]. Furthermore, the good overlap of data in this high frequency range is expected because these polymers differ only in their topology, but not in their chemical composition. This rheological technique in the high frequency range probes local chain properties which are related to segment and entanglement lengths. Thus, the ω_{2x} characteristic frequency in this region changes with polymer composition, as shown in Fig. 3, but does not change if the composition remains the same, as shown in Fig. 6. Therefore, our experimental data are appropriate to be used first as a direct determination of τ_e for PE.

Ferry [4] and Liu [5] empirically established two simple correlations to derive the relaxation time. If Ferry's correlation, according to Eq. (2), is applied, then ω_e is defined from the intersection of G_N^0 with G''. The graphical analysis and determination of τ_e are directly connected to the plateau modulus since the entanglement relaxation frequency increases due to the increase in the plateau modulus. Hence, the plateau moduli must be carefully selected. In our work, we use the value of G_N^0 at 463 K, reported by Ramos *et al.* [6], which is an average value of experimental data and is equal with $2.17 \pm 0.23 \times 10^6$ Pa. Using Ferry's definition and the value of G_N^0, we calculated a τ_e value of $2.5^{+2.5}_{-1.5}$ ns, where the subscript and superscript denotes the error bounds obtained from the error analysis. This means that the entanglement relaxation time is found to be with a probability of 68% within the range defined by the given errors. For a detailed analysis of error bounds, see the supplementary material [29]. The relatively large error range originates from the accuracy of G_N^0 and from the fitting of G'' data. The plateau modulus considered in this work is a mean value with a standard deviation of ~10%. On the other hand, the G'' data points are scattered on the fundamental 3 MHz frequency (Fig. 6). Besides this, after the linear fit of the data points, the parameters which describe the obtained fit are characterized by a relative error of about 9% (intercept's relative error).

Liu's approach, according to Eq. (3), is an alternative approach to identify the magnitude of τ_e experimentally. Using the second crossover (ω_{2x}) a τ_e of $3.0^{+9.0}_{-1.8}$ ns was obtained (for detailed error calculation, see the supplementary material) [29]. In this case, the given error range was even larger than the aforementioned case. The source of this uncertainty is attributed to the errors relating to the fitting procedure of the experimentally determined G' and G'' data points. Nevertheless, the determination of the τ_e was performed with the help of two different approaches, and the values are close to each other. This indicates that the

relaxation times, which were obtained with the help of our QR technique, are reasonable and reliable.

We interpret the results of these two methods as different estimators of one and the same random variable τ_e. This allows calculation of the error bounds of a "pooled sample" from the two "realizations," τ_e^{e} (Ferry's approach) and τ_e^{2x} (Liu's approach). In other words, we define the value and error bounds for τ_e as the average of the two mean values and their errors. The corresponding calculations are presented in the supplementary material [29]. The main result of this paper is as follows: With a probability of 68%, the entanglement relaxation time of PE at 463 K amounts to $\tau_e = 2.8^{+7.6}_{-1.0}$ ns.

We used a calculation method (see Sec. II A), to determine τ_e and found 9 ns at 403 K (see Fig. 5). Using the WLF equation, the value of τ_e was 3.3 ns at 463 K. The relaxation time obtained from calculation is thus in good agreement with the experimentally obtained values.

To verify the results from the high-frequency measurement technique in the following, the value obtained will be compared with data from the literature. Therefore, τ_e-values determined by different techniques from different research groups are presented in Table II. Moreover, the entanglement molecular weights (M_e) were calculated using the following equation [37]:

$$M_e = \frac{4}{5}\frac{\rho_M RT}{G_N^0}, \tag{10}$$

where ρ_M is the melt density, R is the universal gas constant, T is the temperature in K, and G_N^0 is the plateau modulus.

Using the relationship between terminal, τ_t, and entanglement relaxation times [Eq. (5)] as given in Rubinstein and Colby (simplified tube model [50]) and extending it with expression reflecting contour length fluctuation, Ramos *et al.* [6] determined τ_e to be 4.0 ns. Furthermore, they used a simulation method based on Monte Carlo chain dynamics, using a fixed number of 1000 skeletal carbon and 20 chains [6]. In real measurements, these limitations are not adequate. The obtained result for τ_e was 1.3 ns, a value very close to the lower bound of the found interval. Additionally, they determined M_e, 710–880 g/mol, which is lower than the widely used 1000 or 1230 g/mol [6,44,51]. An underestimation of M_e leads to shorter τ_e. This can be seen when their values are compared to our experimental and calculated ones.

In their most recent work, Ramos *et al.* used a molecular dynamics simulation where they extracted information related to mean squared monomer displacements, which allows access to the entanglement relaxation time [6,10]. They found that τ_e at 509 K was equal to 0.8 ns [10]. In the interest of comparison, we shifted this value from 509 to 463 K (using Arrhenius dependency, $E_a = 25$ kJ/mol). As a consequence, the time became 1.4 ns, which is, again, lower than our value.

Another calculation method to determine the τ_e is the dual constraint model [7], an extension of the tube model [50]. The authors used this calculation technique [Eq. (4)] for the determination of the τ_e of HDPE and low density PE (LLDPE). For these materials, 7.0 and 11 ns were found, respectively. Our value is significantly smaller than their results, which may arise from the applied model. Mapping the predictions of dual constraint and double reptation models, they used a C_1 constant which might be responsible for this deviation.

There are other groups, like Chen *et al.*, who developed a method which relates entanglement relaxation time to molecular weight per backbone bond (m_b) [8]. They used two different methods, the bob model and the hierarchical model, both versions of tube model, to quantify the value of τ_e of the LLDPE. Their values amount to ~6 ns for the bob- and ~11 ns for the hierarchical model after shifting them to 463 K. Again, these calculation results are significantly larger than our value. The differences may be attributed to the lower G_N^0 and to the lack of incorporating the contour length fluctuation and constraint release in their models. All these deficiencies can lead to longer relaxation time.

Finally, a completely different technique to determine τ_e experimentally is considered. Richter *et al.* [47,48] used neutron spin-echo spectroscopy (NSE), which gives access to

TABLE II. Values of the plateau modulus, entanglement molecular weight, and entanglement relaxation time of PE at 463 K.

Reference	G_N^0 (MPa) (at 463 K)[a]	M_e[b] (g/mol)	Type of determination (Method)	τ_e (ns)
Present work	Must not be specified!	1100	Experimental[c] (Liu [5])	3.0
	2.17 [6]	1080	Experimental (Ferry [4], empirical)	2.5
	2.1[d]	1120	Calculation TMA model[e]	3.4 (9 at 403 K)
Ramos *et al.* [6,10]	2.04	1150	Calculation[d] (tube model and CLF)	4.0
	2.17	1080	Simulation (molecular dynamics Monte Carlo)	1.3
			Simulation[e] (molecular dynamics)	1.4 (0.8 at 509 K)
Pattamaprom and Larson [7]	2.6	900	Calculation[f] (dual constraint model)	7.0 (HDPE) 11 (LLDPE)
Chen *et al.* [8]	1.97 (at 423 K)	1110	Calculation[e] (Tube model based extrapolation)	6–11.4 (11 up to 21 at 423 K)
Richter *et al.* [47,48]			Experimental[e] (NSE)	9 (5.0 at 509 K)

[a]The different values correspond to different authors.
[b]The melt density was calculated using the following definition: [49] $\rho_M = [1.262 + 9.0 \times 10^{-4}(T - 125)]^{-1}$ with T in °C. The values were up-rounded to 10.
[c]The value of the second cross-over is determined by graphical analysis (Fig. 6) from our measurement and predicted ratio between ω_{2x} and ω_e, as discussed in the text.
[d]Using the value from the given literature.
[e]The value of τ_e at reference temperature (in brackets) using Arrhenius dependency ($E_a = 25$ kJ/mol) was shifted to 463 K.
[f]This value is predicted by the dual constraint model and belongs to different PEs.

the time and space resolved dynamic structure factor S. By application of the Rouse model for short times and the constrained reptation model for longer times to these data, it was possible to determine the basic chain parameters such as friction coefficient and tube diameter. In doing so, the Richter group determined the friction coefficient from the so called "Rouse rate" W ($=\frac{3\cdot k_B T}{\zeta_0 b^2}$), the only fitting parameter to S in the Rouse regime. The tube diameter d was derived from S data in the time region where Q-splitting occurs, Q being the value of the scattering vector. Assuming a certain value of the statistical segment length, τ_e for hydrogenated polybutadiene (essentially a linear, monodisperse PE) at 509 K was determined. Their value of 5 ns was shifted with the help of Arrhenius ansatz and an activation energy of 25 kJ/mol to 463 K, resulting in a value of 9 ns. This value, compared to ours, is significantly larger, but still within the confidence interval. A more recent determination of τ_e by the Jülich group resulted in an even higher value of 7 ns (12.6 ns at 463 K) [52]. The reasons for these significant deviations between the times determined by both techniques become obvious if an alternative to Eq. (1) is considered, which makes the influence of the tube diameter d explicit: $\tau_e = \frac{\xi_0 d^4}{3\pi^2 k_B T b^2}$. It is known from literature [48] that the NSE experiment yields a significantly larger estimate of tube diameter in comparison to the rheology experiment (via determination of plateau modulus), causing the larger τ_e-values stemming from NSE experiments. The origin of this discrepancy remained unclear up till now. Moreover, another part of the difference between the τ_e-values in the literature is due to the use of friction factors stemming from different sources. While Richter *et al.* use $\xi_0 = 4 \times 10^{-13}$ Ns/m at 509 K, which originates from the data of a low molecular weight PE (507 g/mol) in [1], Pearson *et al.* allow the calculation of friction coefficients in dependence of temperature for PE of higher molecular weight (4 kg/mol and higher). This amounts to 12.5×10^{-13} N s/m at 509 K. The results obtained with that equation are in agreement with calculations and experiments given in [2]. Finally, the last source of differences originates from the use of different statistical segment length. While the most authors use the Kuhn length l_K ($= b \cong C_\infty \cdot l_0$, ignoring bond angles) as the statistical segment length, the Jülich group calculates their τ_e-value with $b \cong \sqrt{C_\infty} \cdot l_0$, and l_0 being the C–C bond length. All these effects together explain why the τ_e-values determined by NSE-technique are significantly larger than all other values. On the basis of the presented information, we are not able to decide which technique gives the more accurate τ_e-values.

However, with rheological measurements in the MHz range, it was possible to determine τ_e easily and rapidly, and it does not require the use of expensive instruments such as NSE.

IV. CONCLUSIONS

We have studied the rheological behavior of different types of PE in the kHz- and MHz frequency range to enlarge the accessible frequency range from conventional dynamic rheometers and to show the accuracy of a quartz crystal resonator. On the basis of conventional rheometer measurements and on well investigated reference polymers, we demonstrated good agreement of all these resonator techniques. Our investigations have also shown that the rheological behavior of PE at higher frequencies close to second crossover frequency ω_{2x} is influenced only by the nature of the monomer and not by the branching (topology). The extension of the frequency range and the experimental accessibility of the MHz range, especially in the case of PE, is the most important technical achievement. As a consequence, for the first time, the entanglement relaxation time of PE using high frequency rheometer was determined experimentally from rheological data in the relevant frequency range. We estimated a value of $\tau_e = 2.8^{+7.6}_{-1.0}$ ns at a temperature of 463 K. This value with its error bounds encompasses most of the literature data. Moreover, our results support the idea of Liu [5] of an "experimental definition" for τ_e, which relays on the second cross-point frequency of G^* data and which permits a model free determination of this time. Due to this, this procedure does not rely on the knowledge of entanglement molecular weight and allows the verification of basic chain parameters such as the friction coefficient.

ACKNOWLEDGMENTS

The authors are thankful to Professor Johannsmann for valuable discussions. L.Sz., R.V., and C.F. are grateful to BMBF for financial support within the projects FUNgraphene and CATEFF. D.A. thanks for the support by the EUFP7 Marie-Curie fellowship "SUPRADYN." E.v.R. thanks the Fond National de la Recherche Scientifique for financial support (FNRS, as charge de recherche). The authors are thankful to all reviewers, which helped with their constructive criticism to improve the paper.

References

[1] Pearson, D. S., G. ver Strate, E. von Meerwall, and F. C. Schilling, "Viscosity and self-diffusion coefficient of linear polyethylene," Macromolecules **20**, 1133–1141 (1987).

[2] Luettmer-Strathmann, J., "Segmental mobility of polyolefin melts," Int. J. Thermophys. **22**, 1507–1519 (2001).

[3] van Meerveld, J., "A method to extract the monomer friction coefficient from the linear viscoelastic behavior of linear, entangled polymer melts," Rheol. Acta **43**, 615–623 (2004).

[4] Ferry, J. D., *Viscoelastic Properties of Polymers* (Wiley, New York/Chichester, 1980).

[5] Liu, C.-Y., R. Keunings, and C. Bailly, "Direct rheological evidence of monomer density reequilibration for entangled polymer melts," Macromolecules **40**, 2946–2954 (2007).

[6] Ramos, J., J. F. Vega, D. N. Theodorou, and J. Martinez-Salazar, "Entanglement relaxation time in polyethylene: Simulation versus experimental data," Macromolecules **41**, 2959–2962 (2008).

[7] Pattamaprom, C., and R. G. Larson, "Predicting the linear viscoelastic properties of monodisperse and polydisperse polystyrenes and polyethylenes," Rheol. Acta **40**, 516–532 (2001).

[8] Chen, X., F. J. Stadler, H. Muenstedt, and R. G. Larson, "Method for obtaining tube model parameters for commercial ethene/alpha-olefin copolymers," J. Rheol. **54**, 393–406 (2010).

[9] Likhtman, A. E., and T. C. McLeish, "Quantitative theory for linear dynamics of linear entangled polymers," Macromolecules **35**, 6332–6343 (2002).

[10] Ramos, J., J. F. Vega, and J. Martinez-Salazar, "A new insight into the conformation and melt dynamics of hydrogenated polybutadiene as revealed by computer simulations," Soft Matter **12**, 3929–3936 (2016).

[11] Theobald, S., P. Schwarzenberger, and W. Pechhold, "Measurements of the complex shear modulus of polymers under hydrostatic pressure usina the quartz resonator method," High Pressure Res. **13**, 133–140 (1994).

[12] Kirschenmann, L., and W. Pechhold, "Piezoelectric rotary vibrator (PRV)–A new oscillating rheometer for linear viscoelasticity," Rheol. Acta **41**, 362–368 (2002).

[13] Fritz, G., W. Pechhold, N. Willenbacher, and M. H. Wagner, "Characterizing complex fluids with high frequency rheology using torsional resonators at multiple frequencies," J. Rheol. **47**, 303–319 (2003).

[14] Johannsmann, D., "Studies of viscoelasticity with the QCM," in *Piezoelectric Sensors*, edited by C. Steinem and A. Janshoff (Springer, Berlin/Heidelberger, 2007), pp. 49–109.

[15] Radel, S., and E. Benes, "Utilisation of layered piezoelectric resonators for the online measurement of mass density and viscosity of fluids," Elektrotechn. Informationstechn. **126**, 19–30 (2009).

[16] Sugimoto, I., M. Seyama, and M. Nakamura, "Detection of petroleum hydrocarbons at low ppb levels using quartz resonator sensors and instrumentation of a smart environmental monitoring system," J. Environ. Monit. **1**, 135–142 (1999).

[17] Andersson, M., J. Andersson, A. Sellborn, M. Berglin, B. Nilsson, and H. Elwing, "Quartz crystal microbalance-with dissipation monitoring (QCM-D) for real time measurements of blood coagulation density and immune complement activation on artificial surfaces," Biosens. Bioelectron. **21**, 79–86 (2005).

[18] Johannsmann, D., *The Quartz Crystal Microbalance in Soft Matter Research: Fundamentals and Modeling* (Springer, Cham, Switzerland, 2015).

[19] Wolff, O., and D. Johannsmann, "Shear moduli of polystyrene thin films determined with quartz crystal resonators in the sandwich configuration," J. Appl. Phys. **87**, 4182–4188 (2000).

[20] Johannsmann, D., "Viscoelastic analysis of organic thin films on quartz resonators," Macromol. Chem. Phys. **200**, 501–516 (1999).

[21] Talib, Z. A., Z. Baba, S. Kurosawa, H. Sidek, A. Kassim, and W. Yunus, "Frequency behavior of a quartz crystal microbalance (QCM) in contact with selected solutions," Am. J. Appl. Sci. **3**, 1853–1858 (2006).

[22] Oiseth, S. K., A. Krozer, J. Lausmaa, and B. Kasemo, "Ultraviolet light treatment of thin high-density polyethylene films monitored with a quartz crystal microbalance," J. Appl. Polym. Sci. **92**, 2833–2839 (2004).

[23] Suh, Y. K., B. C. Kim, and Y. H. Kim, "Determination of viscoelastic property in polyethylene crystallization using a quartz crystal resonator," Sensors **9**, 9544–9558 (2009).

[24] Almeida, A., S. Possemiers, M. N. Boone, T. de Beer, T. Quinten, L. van Hoorebeke, J. P. Remon, and C. Vervaet, "Ethylene vinyl acetate as matrix for oral sustained release dosage forms produced via hot-melt extrusion," Eur. J. Pharm. Biopharm. **77**, 297–305 (2011).

[25] Kurek, A. G., "Maßgeschneiderte polyethylen-reaktorblends mit ultra-hochmolekularem polyethylen: Steuerung von materialeigenschaften und nanostrukturbildung durch coträgerung von (post-) Metallocenen," Ph.D. thesis, Universität Freiburg, Germany, 2009.

[26] Kukalyekar, N., R. Huang, S. Rastogi, and J. C. Chadwick, "Are MgCl2-immobilized single-center catalysts for polyethylene really single-center? Confirmation and refutation using melt rheometry," Macromolecules **40**, 9443–9450 (2007).

[27] Honerkamp, J., and J. Weese, "A note on estimating mastercurves," Rheol. Acta **32**, 57–64 (1993).

[28] Winter, H. H., and M. Mours, "The cyber infrastructure initiative for rheology," Rheol. Acta **45**, 331–338 (2006).

[29] See supplementary material at http://dx.doi.org/10.1122/1.4998174 for a comprehensive description of QR set-up, for the used M_w and polydispersity index of EVA copolymers and for thorough discussion about WLF parameters as well as for detailed error calculation.

[30] Kirschenmann, L., *Aufbau einer Quarzresonator-Son de zur Messung der viskoelastischen Eigenschaften von Fluiden und Polymerschmelzen im MHz-Gebiet* (Master Thesis University Ulm, Ulm, 1999).

[31] van Ruymbeke, E., A. Kaivez, A. Hagenaars, D. Daoust, P. Godard, R. Keunings, and C. Bailly, "Characterization of sparsely long chain branched polycarbonate by a combination of solution, rheology and simulation methods," J. Rheol. **50**, 949–973 (2006).

[32] van Ruymbeke, E., R. Keunings, and C. Bailly, "Determination of the molecular weight distribution of entangled linear polymers from linear viscoelasticity data," J. Non-Newtonian Fluid Mech. **105**, 153–175 (2002).

[33] Doi, M., and S. F. Edwards, *The Theory of Polymer Dynamics* (Clarendon, Oxford, 1986).

[34] de Gennes, P. G., "Reptation of a polymer chain in presence of fixed obstacles," J. Chem. Phys. **55**, 572–579 (1971).

[35] Marrucci, G., "Relaxation by reptation and tube enlargement—A model for polydisperse polymers," J. Polym. Sci., Part B **23**, 159–177 (1985).

[36] van Ruymbeke, E., R. Keunings, and C. Bailly, "Prediction of linear viscoelastic properties for polydisperse mixtures of entangled star and linear polymers: Modified tube-based model and comparison with experimental results," J. Non-Newtonian Fluid Mech. **128**, 7–22 (2005).

[37] Larson, R. G., T. Sridhar, L. G. Leal, G. H. McKinley, A. E. Likhtman, and T. C. McLeish, "Definitions of entanglement spacing and time constants in the tube model," J. Rheol. **47**, 809–818 (2003).

[38] van Ruymbeke, E., Y. Masubuchi, and H. Watanabe, "Effective value of the dynamic dilution exponent in bidisperse linear polymers: From 1 to 4/3," Macromolecules **45**, 2085–2098 (2012).

[39] van Ruymbeke, E., V. Shchetnikava, Y. Matsumiya, and H. Watanabe, "Dynamic dilution effect in binary blends of linear polymers with well-separated molecular weights," Macromolecules **47**, 7653–7665 (2014).

[40] Park, S. J., and R. G. Larson, "Dilution exponent in the dynamic dilution theory for polymer melts," J. Rheol. **47**, 199–211 (2003).

[41] Auhl, D., P. Chambon, T. C. B. McLeish, and D. J. Read, "Elongational flow of blends of long and short polymers: Effective stretch relaxation time," Phys. Rev. Lett. **103**, 136001 (2009).

[42] van Ruymbeke, E., C.-Y. Liu, and C. Bailly, "Quantitative tube model predictions for the linear viscoelasticity of linear polymers," Rheol. Rev. **39**, 53–134 (2007).

[43] Park, S. J., P. S. Desai, X. Chen, and R. G. Larson, "Universal relaxation behavior of entangled 1,4-polybutadiene melts in the transition frequency region," Macromolecules **48**, 4122–4131 (2015).

[44] Fetters, L. J., D. J. Lohse, and R. H. Colby, "chain dimensions and entanglement spacings," in *Physical Properties of Polymers Handbook*, edited by J. E. Mark (Springer, New York, 2007), pp. 447–454.

[45] Arsac, A., C. Carrot, and J. Guillet, "Rheological characterization of ethylene vinyl acetate copolymers," J. Appl. Polym. Sci. **74**, 2625–2630 (1999).

[46] Johannsmann, D., "Viscoelastic, mechanical, and dielectric measurements on complex samples with the quartz crystal microbalance," Phys. Chem. Chem. Phys. **10**, 4516–4534 (2008).

[47] Schleger, P., B. Farago, C. Lartigue, A. Kollmar, and D. Richter, "Clear evidence of reptation in polyethylene from neutron spin-echo spectroscopy," Phys. Rev. Lett. **81**, 124–127 (1998).

[48] Richter, D., R. Butera, L. J. Fetters, J. S. Huang, B. Farago, and B. Ewen, "Entanglement constraints in polymer melts—A neutron spin-echo study," Macromolecules **25**, 6156–6164 (1992).

[49] Meissner, J., and J. Hostettler, "A new elongational rheometer for polymer melts and other highly viscoelastic liquids," Rheol. Acta **33**, 1–21 (1994).

[50] Rubinstein, M., and R. H. Colby, *Polymer Physics* (Oxford University, Oxford, NY, 2003).

[51] Ries, M. E., M. G. Brereton, Im. Ward, J. I. Cail, and R. F. Stepto, "Resealing approach to molecular orientation for NMR and optical properties of polymer networks," Macromolecules **35**, 5665–5669 (2002).

[52] Wischnewski, A., M. Monkenbusch, L. Willner, D. Richter, and G. Kali, "Direct observation of the transition from free to constrained single-segment motion in entangled polymer melts," Phys. Rev. Lett. **90**, 58302 (2003).